Hindawi
Journal of Food Processing and Preservation
Volume 2024, Article ID 4506851, 12 pages
https://doi.org/10.1155/2024/4506851

Research Article

Quality Analysis and Shelf-Life Prediction of Antarctic Krill (*Euphausia superba*) Sauce Based on Kinetic Model and Back Propagation Neural Network Model

Hai Chi,[1,2,3] **Yuanxing Zhang**,[1,2] **Lukai Zhao**,[1,3] **Na Lin**,[1] **and Wei Kang**[1]

[1]*East China Sea Fisheries Research Institute, Chinese Academy of Fishery Sciences, Shanghai 200090, China*
[2]*College of Food Science and Engineering, Dalian Ocean University, Dalian 116023, China*
[3]*School of Health Science and Engineering, University of Shanghai for Science and Technology, Shanghai 200093, China*

Correspondence should be addressed to Wei Kang; kangw@ecsf.ac.cn

Received 16 January 2024; Revised 24 March 2024; Accepted 23 April 2024; Published 10 May 2024

Academic Editor: Prakash Bhuyar

The study is aimed at determining how the quality of Antarctic krill (*Euphausia superba*) sauce (AkS) changed over time, including changes in color, moisture content, acid value (AV), peroxide value (POV), thiobarbituric acid reactive substance (TBARS), aerobic plate count, and sensory score. Quality variations and shelf life of AkS were estimated using kinetic model and back propagation (BP) neural network model. The results showed that sensory score, moisture content, and $a*$ values of AkS declined as storage temperature increased at 4, 25, and 37°C. In addition, the $L*$ values, $b*$ values, AV, POV, and TBARS of AkS increased as storage duration increased, indicating that high storage temperature of the samples accelerated quality degradation. The primary reason for AkS degradation was the oxidation of proteins and lipids. The POV, TBARS, and total sensory evaluation rating exhibited a highly significant correlation, and therefore, POV and TBARS were selected as the indicators for the two models. The BP neural network outperformed the kinetic model in predicting quality changes over the whole storage period, with relative errors of less than 10%. In terms of shelf-life prediction, the BP neural network's relative errors were 11.76% and 13.39% in POV and TBARS, respectively. POV and TBARS had experimental shelf lengths of 119 and 142 d, respectively. Compared with the kinetic model, the BP neural network model predicted the quality changes and shelf life of AkS with greater accuracy and stability. The findings offer fundamental insights and innovative concepts for the production of high-value Antarctic krill products, as well as the exploitation of Antarctic krill resources.

1. Introduction

Antarctic krill (*Euphausia superba*) is a shrimp-like creature found in the Antarctic Ocean [1]. Its biomass is estimated to be 400–1550 million metric tons, which serves as the most important animal protein resource for both marine animals and humans [2]. Antarctic krill proteins contain all of the essential amino acids [3]. They meet Food and Agriculture Organization/World Health Organization human consumption requirements and have a high biological value [4]. Antarctic krill lipids are abundant in omega-3 polyunsaturated fatty acids, such as eicosapentaenoic acid, docosahexaenoic acid, phospholipids, and astaxanthin [5]. Bioactive peptides, on the other hand, such as Ca-chelating peptides, antioxidant peptides, and antihypertensive peptides from Antarctic krill, also have been produced [6–9]. Thus, its widespread availability and high nutritional value have the potential to ease the scarcity of marine resources. The number of Antarctic krill products on the market has increased, and they are primarily used in aquaculture, medication, and healthcare [7]. Although most Antarctic krill is used to make aquatic feed, which has low economic value, humans consume approximately 12% of the total Antarctic krill via backward processing [8]. Therefore, the creation of high-value commercial products is desperately needed. Many methodological investigations are being conducted in order to promote the consumption and usage of Antarctic krill as a high-value component of human meals.

The abundant Antarctic krill resources could be used to produce significant quantities of Antarctic krill sauce (AkS) [10]. AkS is a flavorful, ready-to-eat aquatic product with high nutritional value, which outweighs the disadvantage of inconvenient storage. Because of the abundance of seafood, the AkS spoils fast owing to high quantities of protein and unsaturated fatty acids. During storage, AkS is susceptible to lipid oxidation, protein denaturation, the Maillard reaction, and astaxanthin degradation [11–13]. These elements lead to loose texture, poor color, off-flavor development, and rancidity, all of which have a direct influence on shelf life. As a result, the product is susceptible to gradual degradation during storage.

The spoilage of AkS during storage prevents Antarctic krill resources from being used efficiently. To maintain food safety and quality, the food sector must predict quality changes during storage [14]. It is critical to identify the key signs and develop a shelf-life prediction model. The Arrhenius equation is a typical chemical kinetic model that can predict the changes in food quality changes at various storage temperatures [15]. Many studies on the kinetic model based on the Arrhenius equation have been conducted to predict the shelf life of foods such as rabbit meat [16], beef [17], and pork sausage [18]. Most previously investigated kinetic models have been applied to relatively simple meals. However, owing to the complicated composition of AkS, the quality variations of AkS during storage are diversified. The Arrhenius equation is often applicable only to a narrow temperature range [19], and the kinetic model contains certain flaws. The prediction of AkS quality variations during storage necessitates a model with greater generalization ability and improved prediction accuracy. Back propagation (BP) neural network model is a new food quality prediction methodology [20]. BP neural network is currently widely employed in the food industry for the categorization of food species and quality, element content detection, and risk management [21]. To date, single kinetic models or BP neural networks have been used to estimate the shelf life of foods. Few studies have compared the prediction accuracy of kinetic models with that of BP neural network models. Fu et al. [22] used the BP neural network approach to develop a *Tricholoma matsutake* prediction model to quantify the association between quality indices and remaining shelf life. Based on protein degradation, Zhu et al. [23] discovered that the BP neural network has tremendous promise in forecasting the quality of dry-cured ham. These studies showed that utilizing a BP neural network to forecast the quality change and shelf life of AkS is feasible. To date, single kinetic models or BP neural networks have been used to estimate the shelf life of foods. Few studies have compared the prediction accuracy of the kinetic model with that of BP neural network models. Thus, research is required to determine which model has the best predictive performance for AkS and to select a better model for development and prediction.

The primary goals of this experiment were as follows: (I) determine the color difference, water content, acid value (AV), peroxide value (POV), thiobarbituric acid reactive substance (TBARS), and aerobic plate count variations of AkS held at 4, 25, and 37°C; (II) use the Arrhenius model and the BP neural network to create a shelf-life prediction model for AkS at various storage temperatures; and (III) compare the prediction performance for the two models. The study is aimed at providing concepts and fundamental facts regarding the use of AkS in the creation of high-value commercial products.

2. Materials and Methods

2.1. Sample Collection. The Antarctic krill was collected at the FAO48.6 region of the Antarctic Ocean in January 2022. All the Antarctic krill samples were delivered to the laboratory in May and stored at -80°C before use. The garlic, millet spicy, dried pepper, cooking oil, and Jinhua ham were purchased from the supermarket in Shanghai, China.

2.2. Preparation of AkS. About 100 g of complete raw Antarctic krill without blackhead was selected and thawed. The thawed Antarctic krill were then immersed in boiling water for 3 min and then drained at room temperature until the water content was no more than 35%. Subsequently, the dried Antarctic krill was placed in a sterile bag (76 × 127 mm, BKMAN, Beijing, China) at 4°C overnight to balance the water in the Antarctic krill. The Antarctic krill with individual sizes ranging from 3 to 5 cm were crushed in the cooking equipment (Chigo, ZG-L74A, Guangzhou, China), and those less than 3 cm in length were immediately combined with crushed shrimp at a 3 : 5 (g/g) ratio. The Jinhua ham was roasted for 15 min before being chilled and shredded. In the cooking machine, the garlic, millet spicy, and dried pepper were smashed. A small volume of cooking oil was heated before adding the garlic, millet spicy, and dried pepper. After stirring for 5 min, the mixture was combined with Antarctic krill and Jinhua ham and stirred for another 10 min. Seasonings were included into the mixture, which was stirred for another 5 min. Throughout the procedure, the oil temperature was kept at less than 130°C.

2.3. Experimental Description. AkS was kept in sterilized 50 mL glass bottles at 4, 25, and 37°C. Every 7 days, duplicate sauce samples were collected to analyze color difference, moisture content, AV, POV, TBARS level, aerobic plate count, and sensory assessment.

2.4. Color Difference Detection. Color difference was determined as described by Kim et al. [24]. Color variations were assessed using CIELAB color space coordinates ($L*$, $a*$, and $b*$) measured using a CM-700d (Konica, Japan, Shanghai iBetter Technology Co., Ltd.) colorimeter at room temperature.

2.5. Water Content Detection. Water content was determined using the technique developed by Rønholt et al. [25]. Briefly, a 5 g sample was put in a porcelain crucible. The samples were incubated at 100°C for 6 h before cooling for 30 min at room temperature in a zeroed dish. The percentage difference before and after water evaporation was used to compute the water content.

2.6. Lipid Extraction. For total lipid extraction from AkS, a modified method by Harrison and Watts [26] was used. Briefly, 10 g of the material was put into an Erlenmeyer flask (As One, 200 mL, Beijing, China). The materials were mixed with 50 mL petroleum ether (Sigma-Aldrich, Shanghai, China) and left to extract for at least 12 h. The filtered extract was then evaporated (YMD-60, YHCHEM, Shanghai, China) (40°C, 55 rpm, 30 min) to remove the petroleum ether. The fat in the Erlenmeyer flask was collected and stored at -18°C for one week for subsequent examination.

2.7. AV Detection. AV measurement was conducted as described by Guo et al. [27]. Briefly, about 1 g of each fat extract was dissolved in isopropanol/diethyl ether (Sigma-Aldrich, Shanghai, China) solution and titrated to the phenolphthalein (Sigma-Aldrich, Shanghai, China) endpoint using 0.1 mol/L potassium hydroxide solution (Sigma-Aldrich, Shanghai, China). The AV value was expressed as milligrams of potassium hydroxide consumed for per gram of sample.

2.8. POV Detection. The POV was calculated using the approach described by Cebi et al. [28], with slight modifications. In a flask, 1 g of each AkS sample was dissolved in 10 mL of chloroform (Sinopharm Chemical Reagent Co., Ltd., Shanghai, China). The flask was filled with 15 mL of glacial acetic acid (Sinopharm Chemical Reagent Co., Ltd., Shanghai, China) and 1 mL of potassium iodide saturated solution (Sinopharm Chemical Reagent Co., Ltd., Shanghai, China). The flask was closed and placed in a dark area for 5 min after being shaken with a hand for 1 min. After adding 15 mL of distilled water, the mixture was titrated against 0.01 mol/L sodium thiosulphate solution (Sigma-Aldrich, Shanghai, China) using starch solution (Aladdin, Beijing, China) as the indicator. Under the same settings, a blank was also titrated. The peroxide equivalent to iodine mass fraction (g/100 g) was used to calculate the POV.

2.9. TBARS Detection. TBARS were calculated in the manner reported by Fan et al. [29], with minor modifications. Approximately 10 g of AkS samples was combined with 100 mL of 7.5% trichloroacetic acid stock solution (Sinopharm Chemical Reagent Co., Ltd., Shanghai, China) and stirred. The sample was shaken for 30 min at 50°C before being centrifuged at 5000 rpm for 10 min at 4°C (Eppendorf, Centrifuge 5810R, Germany). Following that, the filtrate was diluted to 100 mL with distilled water. The aforesaid 5 mL diluent was combined with 20 mM TBA solution, and the combination was boiled on boiling water for 10 min. The sample was brought to room temperature. Absorbance (Abs) was measured in a microplate reader (Biotek, PowerWave XS, USA) at 532 nm. The following methods were used to get TBARS:

$$\text{TBARS (mg/kg)} = \frac{\text{Abs} - 0.04979}{1.125063}. \quad (1)$$

2.10. Aerobic Plate Count Detection. Samples (5 g) were mixed with 45 mL of sterile saline to prepare a sample homogenate. The contents were sequentially diluted to obtain homogenates. After resting for 30 min, 100 μL of each homogenate was absorbed onto the corresponding plate containing plate count agar medium, and the mixture was rotated to mix the contents. After 48 h of incubation at 37°C, the total number of colonies was counted. Data were recorded as colony-forming units (CFU) and expressed as log CFU/g.

2.11. Sensory Evaluation. Ten instructors with typical taste sensitivity and a basic sensory evaluation background evaluated the AkS. The participants were taught how to assess the samples using the sensory evaluation criteria (Table 1).

2.12. Development of Kinetic Models. Physical and chemical interactions, as well as microbiological activities, may alter the quality of food during storage. Most food quality changes during preparation and storage followed zero- or first-order reaction [30]. The zero- (Equation (2)) and first-order (Equation (3)) kinetic models were used for the exponential regression analysis. The kinetic model used in this experiment was determined by the regression equation's determination coefficient. The shelf-life prediction model was created using the Arrhenius equation and the kinetic model. The zero- and first-order reaction equations are as follows:

$$B = B_0 - kt, \quad (2)$$

$$B = B_0 e^{kt}. \quad (3)$$

The Arrhenius equation (Equation (4)) describes the chemical reaction [30]. The model using temperature as an independent variable elucidates the link between the chemical reaction rate (K) and the absolute temperature (T). The model can accurately depict the rate of food deterioration. At three different storage temperatures, E_a and the finger front factor k_0 may thus be derived from the rate constant k. The equation is written as follows:

$$\ln k = \frac{-E_a}{RT} + \ln k_0. \quad (4)$$

Equations (2) and (4) were converted to obtain the formula for the shelf-life (SL, days) prediction model of AkS:

$$\text{SL} = \frac{|B_0 - B|}{k_0 e^{(-E_a/RT)}}. \quad (5)$$

Equations (3) and (4) were also converted to obtain the formula for the SL prediction model of AkS:

$$\text{SL} = \frac{\ln (B/B_0)}{k_0 e^{(-E_a/RT)}}, \quad (6)$$

where B and B_0 are the levels of quality indicators at storage time t (d) and initial value; k and k_0 are reaction rate constants and pre-exponential factor, respectively; and E_a, T, and R are the activation energy, absolute temperature, and molar gas constant (8.3144 JK^{-2}/mol), respectively.

2.13. Development of BP Neural Network. To increase the BP neural network prediction accuracy, the tansig and purelin functions were used as activation functions at the input

Table 1: Criteria for the sensory evaluation of AkS.

Index	Criteria		
Color	Slightly gray No shine	Slightly red Slightly shine	Bright red Color is fresh and shiny
Aroma	None Serious peculiar smell	Faint Has faint seafood odor Slightly peculiar smell	Ample Strong seafood odor No peculiar smell
Texture	Loose Unevenly distributed	Slightly uniform Slightly loose	Tight and uniform
Grade	Bad (0-4)	General (5-7)	Good (8-10)

and output layers, respectively [24]. The BP neural network accepts two inputs (temperature and storage duration) and produces two outputs (POV and TBARS level). The number of hidden layer neurons was set at ten using empirical formulae and a trial-and-error method [31, 32]. The BP neural network topology was tuned to type 2-10-1 to replicate the quality fluctuations of AkS during storage at various temperatures. The mapminmax function was used to standardize the input data in order to decrease data variance and enhance the model's convergence speed and stability of the model. The training goal error was set to 0.00001. The learning rate was set to 0.01, and the number of training steps was limited to 1000. Finally, the mean square error (MSE) was utilized to assess the BP neural network's prediction ability of the BP neural network.

2.14. Statistical Analysis. All experimental data were collected at least three times. Raw data was analyzed using Microsoft Excel 2016 and reported as mean ± standard deviation. SPSS software (version 24.0, SPSS, Chicago, IL, USA) was used for analysis of variance, and Duncan's multiple range test was used to evaluate significant differences at $P < 0.05$. A BP neural network model was performed using MATLAB R2017b software.

3. Results and Discussion

3.1. Color Difference Analysis. The $L*$, $a*$, and $b*$ values varied from 24.55 ± 0.31 to 27.72 ± 0.29, 22.51 ± 0.04 to 1.65 ± 0.05, and -13.64 ± 0.07 to -11.85 ± 0.21, respectively (Table 2). There was no significant change in the $L*$ value ($P > 0.05$) during the initial stages of storage. However, at the three storage temperatures, the $L*$ values of AkS samples grew considerably after 70 d ($P < 0.05$) as the storage period increased. Ran et al. [33] proposed that an increase in $L*$ value is due to the denaturation of myofibrillar and sarcoplasmic proteins, which destroys the protein structure. Consequently, the free water content and surface light reflectance of the AkS samples increased.

The $a*$ values of AkS decreased as storage duration increased, which could be attributed to lipid oxidation and pigment loss during storage [34, 35]. As shown in Table 2, after 70 d of storage at 4, 25, and 37°C, the $a*$ values of the samples decreased from 2.51 to 1.91, 1.71, and 1.65, respectively. According to Cassens et al. [36], high storage temperature promotes color changes. The higher the storage temperature in this study, the faster the decrease in the $a*$ value. In contrast, as storage time increased, so did the $b*$ values.

The $b*$ values of the samples increased from -13.64 to -12.30, -12.21, and -11.85 after 70 d of storage at 4, 25, and 37°C, respectively, as shown in Table 2. Chelh et al. [37] reported that the formation of a Schiff pigment (lipofuscin) during lipid and protein oxidation increases the $b*$ value of meat products, which might explain the results.

3.2. Moisture Content Analysis. Figure 1(a) indicates that the moisture content of AkS reduced as storage time increased. After 70 d of storage, the moisture content of the samples fell from 18.8% to 6.9%, 5.9%, and 5.2% at 4, 25, and 37°C, respectively. This reduction in moisture content might be attributed to the oxidation of proteins in the AkS as the storage duration increased. This oxidation destroys the internal tissue structure and decreases the water binding ability of myofibrillar protein to be reduced [38].

3.3. AV Analysis. The AV of the product represents the degree of lipid breakdown and rancidity during storage. Higher AV values correspond to larger quantities of free fatty acids produced by lipid hydrolysis [39]. Antarctic krill has an excessive amount of fat, and the AkS processing was carried out with heat treatment, which contributed to fat oxidation and expedited the increase in primary oxidation. The initial value of AV for AkS was 0.65 mg/g, as shown in Figure 1(b). After 70 d of storage, the AV of the sauce samples increased to 1.42 mg/g at 4°C. The samples at higher temperatures had a more rapid increase in AV ($P < 0.05$) than of the sample at 4°C. After 70 d, the AV of sauce samples at 25 and 37°C grew to 1.94 and 2.45 mg/g, respectively, which was substantially greater ($P < 0.05$) than that of the sample at 4°C. Hernández Becerra et al. discovered that shrimp experience lipid hydrolysis and oxidation during the heat treatment procedure [40]. According to Soto-Rodríguez et al. [41], the drying process also causes oxidation in shrimp, which can be cytotoxic, mutagenic, and carcinogenic. Their results of changes in acid value in shrimp throughout processing are consistent with our findings.

3.4. POV Analysis. The principal products generated at the start of a lipid autoxidation process are peroxides, which represent the degree of primary lipid oxidation. The chemical degrades into odorous volatile molecules such as

Table 2: Changes in the color differences of AkS at different storage temperatures.

Temperature (°C)	Storage time (d)	$L*$	$a*$	$b*$
4°C	0	24.55 ± 0.31^{a}	2.52 ± 0.04^{a}	-13.64 ± 0.07^{a}
	7	24.93 ± 0.06^{b}	2.37 ± 0.03^{b}	-13.55 ± 0.04^{ab}
	14	24.92 ± 0.14^{b}	2.33 ± 0.06^{b}	-13.48 ± 0.06^{b}
	21	25.09 ± 0.25^{b}	2.26 ± 0.01^{c}	-13.40 ± 0.09^{bc}
	28	25.61 ± 0.14^{cd}	2.25 ± 0.05^{c}	-13.32 ± 0.02^{c}
	35	25.47 ± 0.05^{c}	2.23 ± 0.01^{cd}	-13.20 ± 0.07^{cd}
	42	25.90 ± 0.09^{d}	2.18 ± 0.04^{d}	-13.18 ± 0.0^{d}
	49	27.39 ± 0.42^{e}	2.13 ± 0.01^{de}	-12.98 ± 0.15^{e}
	56	27.37 ± 0.15^{e}	2.09 ± 0.04^{ef}	-12.71 ± 0.05^{f}
	63	26.92 ± 0.04^{f}	2.01 ± 0.05^{f}	-12.47 ± 0.08^{g}
	70	26.91 ± 0.09^{f}	1.91 ± 0.02^{g}	-12.30 ± 0.03^{h}
25°C	0	24.55 ± 0.31^{a}	2.52 ± 0.04^{a}	-13.64 ± 0.07^{a}
	7	25.02 ± 0.09^{b}	2.35 ± 0.02^{b}	-13.53 ± 0.02^{b}
	14	24.89 ± 0.30^{b}	2.31 ± 0.06^{b}	-13.45 ± 0.04^{b}
	21	24.99 ± 0.14^{b}	2.25 ± 0.04^{c}	-13.34 ± 0.03^{c}
	28	25.66 ± 0.15^{c}	2.22 ± 0.06^{c}	-13.28 ± 0.12^{c}
	35	24.96 ± 0.03^{b}	2.18 ± 0.03^{cd}	-13.16 ± 0.04^{d}
	42	24.78 ± 0.02^{ab}	2.10 ± 0.04^{d}	-13.00 ± 0.03^{e}
	49	26.69 ± 0.11^{d}	2.02 ± 0.09^{de}	-12.62 ± 0.08^{f}
	56	27.12 ± 0.06^{ef}	1.98 ± 0.05^{e}	-12.42 ± 0.08^{g}
	63	27.37 ± 0.05^{e}	1.81 ± 0.03^{f}	-12.33 ± 0.08^{g}
	70	27.01 ± 0.15^{f}	1.71 ± 0.05^{g}	-12.21 ± 0.02^{h}
37°C	0	24.55 ± 0.31^{a}	2.52 ± 0.04^{a}	-13.64 ± 0.07^{a}
	7	24.63 ± 0.05^{a}	2.32 ± 0.06^{b}	-13.48 ± 0.07^{ab}
	14	24.49 ± 0.11^{a}	2.29 ± 0.01^{bc}	-13.38 ± 0.03^{bc}
	21	25.11 ± 0.14^{bc}	2.23 ± 0.08^{bcd}	-13.31 ± 0.06^{bc}
	28	24.96 ± 0.07^{b}	2.21 ± 0.05^{cd}	-13.24 ± 0.07^{cd}
	35	25.33 ± 0.17^{c}	2.17 ± 0.02^{d}	-13.10 ± 0.03^{d}
	42	26.22 ± 0.19^{d}	2.03 ± 0.07^{e}	-12.74 ± 0.08^{e}
	49	26.90 ± 0.20^{e}	1.91 ± 0.01^{f}	-12.55 ± 0.03^{f}
	56	27.45 ± 0.20^{fg}	1.78 ± 0.04^{g}	-12.06 ± 0.05^{g}
	63	27.22 ± 0.06^{f}	1.72 ± 0.05^{gh}	-11.95 ± 0.19^{gh}
	70	27.72 ± 0.29^{g}	1.65 ± 0.05^{h}	-11.85 ± 0.04^{h}

Note: different letters in superscript following the average ± deviation in a column indicate significant differences ($P < 0.05$).

alcohols, ketones, and aldehydes. As a result, POV measurement can be used to assess the degree of oxidative degradation of the product [39]. As shown in Figure 1(c), the POV of AkS at different storage temperatures rose with storage duration, from 0.03 to 0.11 g/100 g at 4°C, 0.15 g/100 g at 25°C, and 0.16 g/100 g at 37°C. After 70 d, the samples at 4°C were considerably lower ($P < 0.05$) than the samples at 25 and 37°C, demonstrating that low temperature may effectively suppress lipid oxidation and extend the shelf life of the product. The faster rate of POV development at 25 and 37°C might be attributed to the greater storage temperature, which decreases the activation energy for free fatty acid oxidation.

3.5. TBARS Analysis. The quantity of malondialdehyde in TBARS represents the degree of oxidative breakdown of polyunsaturated fatty acids during lipid oxidation. TBARS are commonly used to determine the oxidation state of numerous meat products [42]. Malondialdehyde has an odor and emits unpleasant fumes when TBARS levels exceed 2.0 mg/kg [43]; hence, TBARS levels are helpful in evaluating the degree of oxidation of foods. The AkS had an initial TBARS of 0.74 mg/kg, which rose to 1.18, 1.31, and 1.39 mg/kg after 70 d of storage at 4, 25, and 37°C, respectively. Figure 1(d) showed that the higher the temperature, the faster the TBARS of the sauce samples increased. These phenomena corresponded to the AV and POV because the increased temperature might have increased the production of free radicals and enhanced the breakdown and polymerisation of hydroperoxides, resulting in the fast oxidation of meat items in AkS samples [44]. TBARS levels in dried shrimp increased during accelerated storage, according to Li et al. [45].

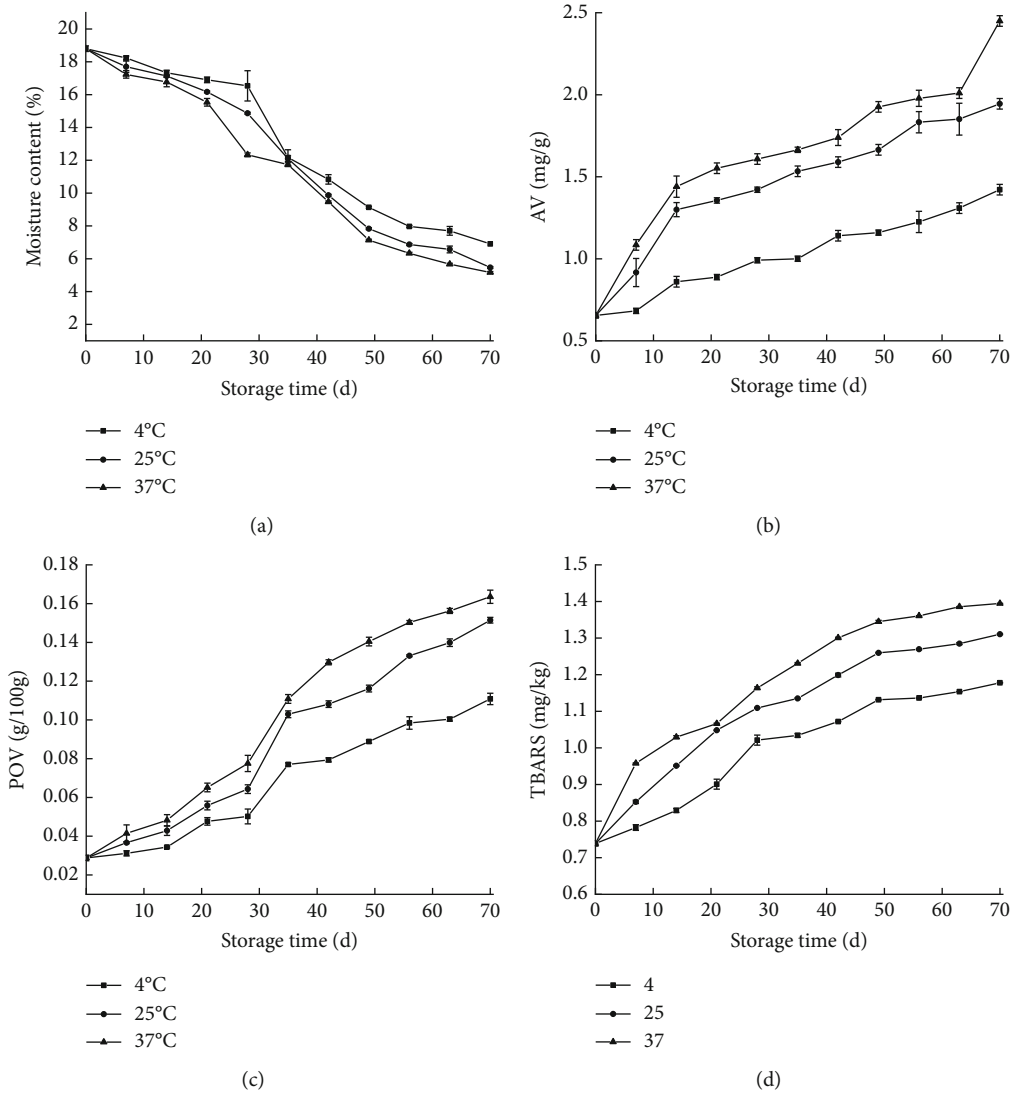

Figure 1: Changes in (a) moisture content, (b) AV, (c) POV, and (d) TBARS of AkS at different temperatures during the storage time.

3.6. Aerobic Plate Count. The aerobic plate count of the AkS samples remained undetectable after 56 d of storage at various temperatures, as shown in Table 3. It might be attributed to the high temperature and commercially sterile production environment. The highly salt- and water-deficient environment of the AkS system may also hinder the development of microorganisms [45]. As a result, the microbial influence on the product was minimal. In this study, the major causes of degradation during food storage were protein and fat oxidation.

3.7. Sensory Evaluation. Sensory qualities are strongly associated with physicochemical parameters during storage, and sensory attributes represent the quality changes that occur in foods during storage [46]. A score of less than 4 indicates that the color, texture, and scent of the AkS have deteriorated. The AkS was initially scarlet and shiny, with a potential and harmonious seafood flavor and a homogeneous texture, as shown in Figure 2. The bright red AkS became somewhat gray in the latter stages of preservation. The texture of the AkS got looser as storage time increased. The texture scores of the samples declined from 8.5 to 3.3 and 2.3 after 70 d of storage at 25 and 37°C, indicating sample texture degradation. Moreover, the texture scores at 25 and 37°C were considerably lower ($P < 0.05$) than the sample at 4°C. The scent score also declined as the storage duration increased. The occurrence was linked to the oxidation of aroma-producing chemicals in the samples as storage time increased [34]. The decreases in the scent score was quicker when the storage temperature was higher, which is consistent with the texture and color scores. Lower temperatures reduced the deterioration of the sensory quality of the AkS samples after storage.

3.8. Prediction Models for AkS

3.8.1. Correlation Analysis of the Indicators. The Pearson correlation coefficients between indicators were strong at various storage temperatures. Except for the aerobic plate count, all indices of AkS exhibited a very significant

Table 3: Changes in the aerobic plate count of AkS at different storage temperatures.

Storage time (d)	4°C (CFU/g)	25°C (CFU/g)	37°C (CFU/g)
0	ND	ND	ND
56	ND	ND	ND
63	<30	<30	<30
70	<30	<30	<30

Note: ND means not detected.

association ($P < 0.01$). According to the findings, the oxidation of lipids and proteins was the primary cause of AkS deterioration. The correlation coefficients between POV and overall sensory ratings were 0.951, 0.986, and 0.979 at 4, 25, and 37°C, whereas those between TBARS level and total sensory ratings were 0.897, 0.933, and 0.923 at 4, 25, and 37°C. The POV, TBARS level, and total sensory ratings had a significant correlation. As a result, POV and TBARS were used to construct a thorough model of the shelf life of AkS during storage at 37°C.

3.8.2. Establishment of Kinetic Models Based on the POV and TBARS Level. The Arrhenius equation has been widely utilized in food research to measure the influence of temperature on the rates of various of chemical and biological processes, as well as microbial growth and inactivation [16]. The experimental data were fitted by swapping zero- and first-order kinetic models. As shown in Table 4, the $\sum R^2$ fitted to the zero-order kinetic equation during storage was higher than the $\sum R^2$ fitted to the first-order kinetic equation for both the POV and TBARS level. According to these findings, variations in the POV and TBARS level in AkS were more compatible with the zero-order chemical reaction kinetic model. Therefore, the zero-order kinetic model can replicate the quality fluctuations of AkS.

Calculating $\ln k$ vs. $1/T$ using the reaction rate constants k and storage temperature T for the three temperatures in Table 4 yielded a linear regression equation. The pre-exponential factor E_a for POV and TBARS level were 9452.19 kJ/mol and 11082.56 kJ/mol, respectively, as shown in Table 4. The POV and TBARS level had activation energies k_0 of 0.085 and 0.506, respectively. The R^2 values of the Arrhenius regression equations for the POV and TBARS level at various storage temperatures were 0.985 and 0.987, suggesting a good fit to the linear equation.

3.8.3. Establishment of BP Neural Network Based on POV and TBARS. The experimental data on changes in the POV and TBARS level of AkS during storage at 4, 25, and 37°C were used to train the BP neural network, and the results are shown in Figure 3. The MSE began to reduce and stabilize as the number of training steps increased. In the second and fifteenth phases, the POV and TBARS level achieved ideal validation performances of 0.005. The whole set of training, testing, and validation correlation coefficients was all more than 0.98. The POV and TBARS level had overall correlation values of 0.98 and 0.99, respectively. According to the results, the created BP neural network did not exhibit an underfitting state [47], and the optimized model and the experimental data are well matched.

3.9. Comparison of Kinetic Model and BP Neural Network. Table 5 shows the relative errors between the predicted and experimental data of 310.15 K generated to test the reliability and accuracy of the two models. According to Kaymak-Ertekin et al. [47], only models with relative errors of less than 10% are acceptable. The relative errors of the Arrhenius model based on the POV exceeded 10% at 14, 21, and 28 d, as shown in Table 5. The deviation from the linear zero-level kinetic equation might be attributed to the rapid oxidation of the product at the start of storage of the sauce at 37°C. Kinetic models have been commonly utilized to predict the shelf life of many products, including aquatic products, fruits, and sauerkraut [46, 48, 49]. Several studies found that the Arrhenius model may accurately reflect the changes in quality indexes [46, 48]. When several quality indicators, such as colors and total acid, were used to estimate shelf life, the relative errors ranged from 10% to 15%, especially at higher temperatures. These findings were comparable to those from our study. From 7 to 70 d, the kinetic model predicted the TBARS level of AkS with high accuracy, with relative errors within 10%. Table 5 reveals that the BP neural network model had fewer relative errors than the kinetic model. Throughout the storage time, the relative error of the BP neural network model was less than 10% for both the POV and the TBARS, and it was more stable.

To evaluate the dependability of the two models, the shelf life of AkS using the two indicators were determined. The maximum permissible levels for the samples were 0.25 g/100 g and 2 mg/kg for the POV and TBARS level, respectively. The kinetic models used for the shelf-life prediction using the POV and TBARS values were produced using the following equations.

$$\mathrm{SL}_{\mathrm{POV}} = \frac{|B_0 - B|}{0.085 \times \exp\left(-9452.19/RT\right)}, \tag{7}$$

$$\mathrm{SL}_{\mathrm{TBARS}} = \frac{|B_0 - B|}{0.506 \times \exp\left(-11082.56/RT\right)}. \tag{8}$$

The experimental shelf lives of the POV and TBARS were 119 and 142 d, respectively, as shown in Table 6. The shelf lives of AkS determined using kinetic models in POV and TBARS were 101 and 183 d, respectively. Each point at 37°C from 70 to 200 d was swapped into the trained BP neural network for shelf-life prediction at 7-day intervals. As shown in Table 6, the relative error of the BP neural network was lower than that of the kinetic model for each index. Some of the high kinetic model prediction discrepancies might be attributed to the complex material composition of AkS and the uncertainty of lipid oxidation during storage. It made the Arrhenius model important for accurately predicting shelf life. These findings are consistent with those reported by Du et al. [46]. In conclusion, the BP neural network outperformed the Arrhenius model in terms of prediction performance during storage.

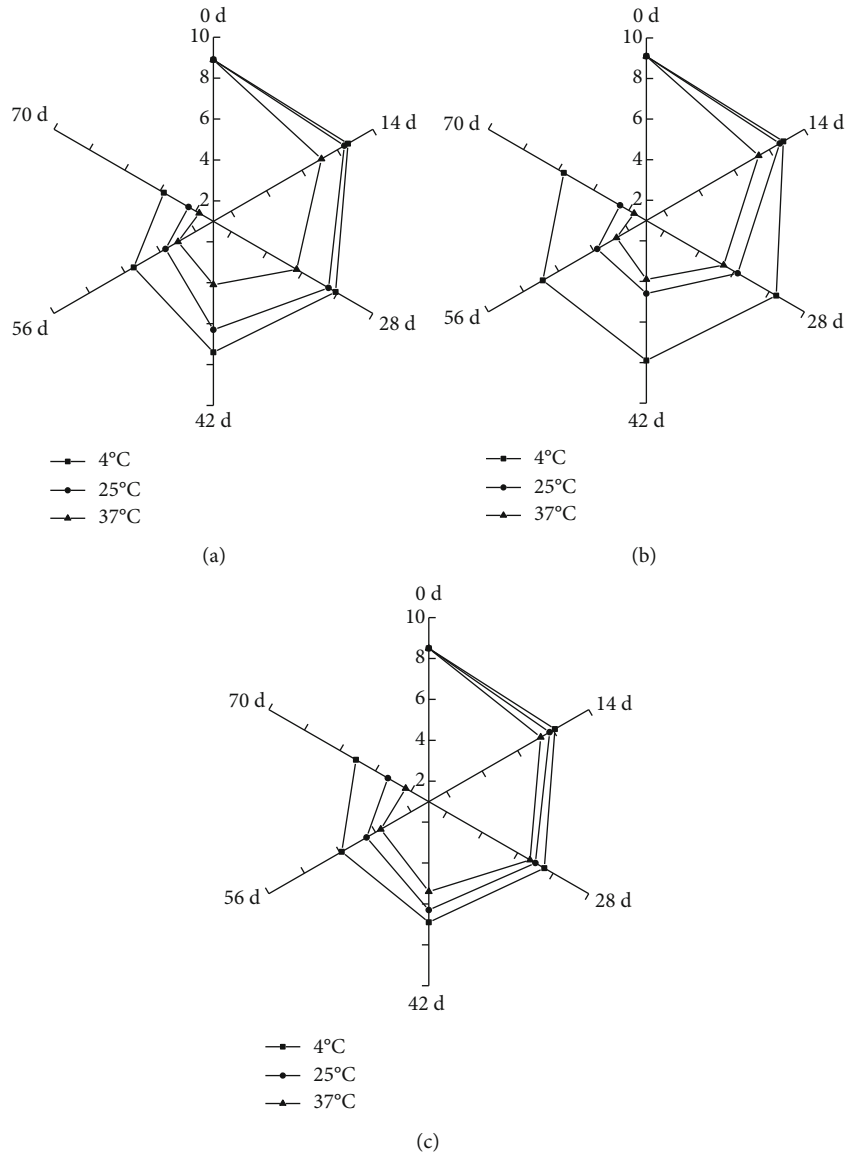

Figure 2: Changes in the sensory value of AkS at different storage temperatures. (a)–(c) represent color, aroma, and texture, respectively.

Table 4: Kinetic model parameters for quality changes in AkS at different storage temperatures.

Indicators	Temperature (°C)	Zero-order model			First-order model		
		k	R^2	$\sum R^2$	k	R^2	$\sum R^2$
POV	4	0.00139	0.9621	2.9316	0.02032	0.9087	2.7837
	25	0.00193	0.9935		0.02296	0.9663	
	37	0.00213	0.9760		0.01943	0.9087	
Arrhenius equation				$\ln k = -1136.9x - 2.4661$			
TBARS level	4	0.00408	0.8358	2.8756	0.00356	0.8115	2.8839
	25	0.00598	0.9261		0.00493	0.9060	
	37	0.00673	0.9280		0.00527	0.9017	
Arrhenius equation				$\ln k = -1333.0x - 0.6806$			

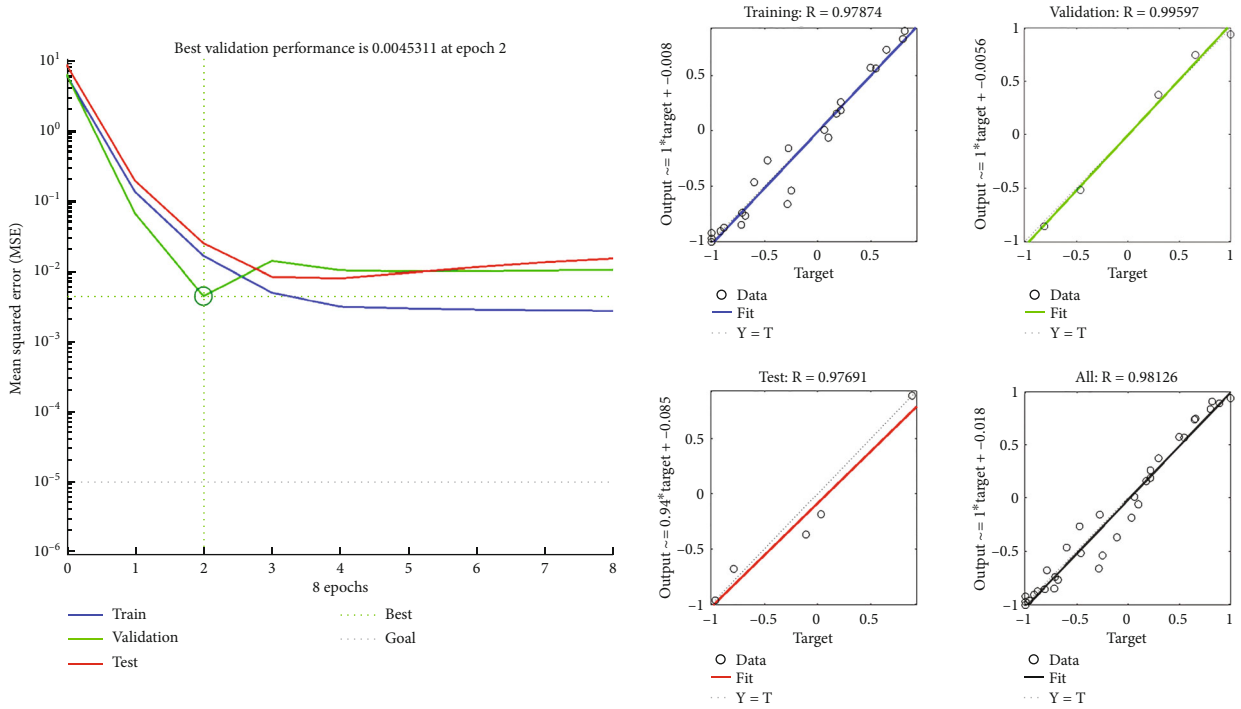

(POV)

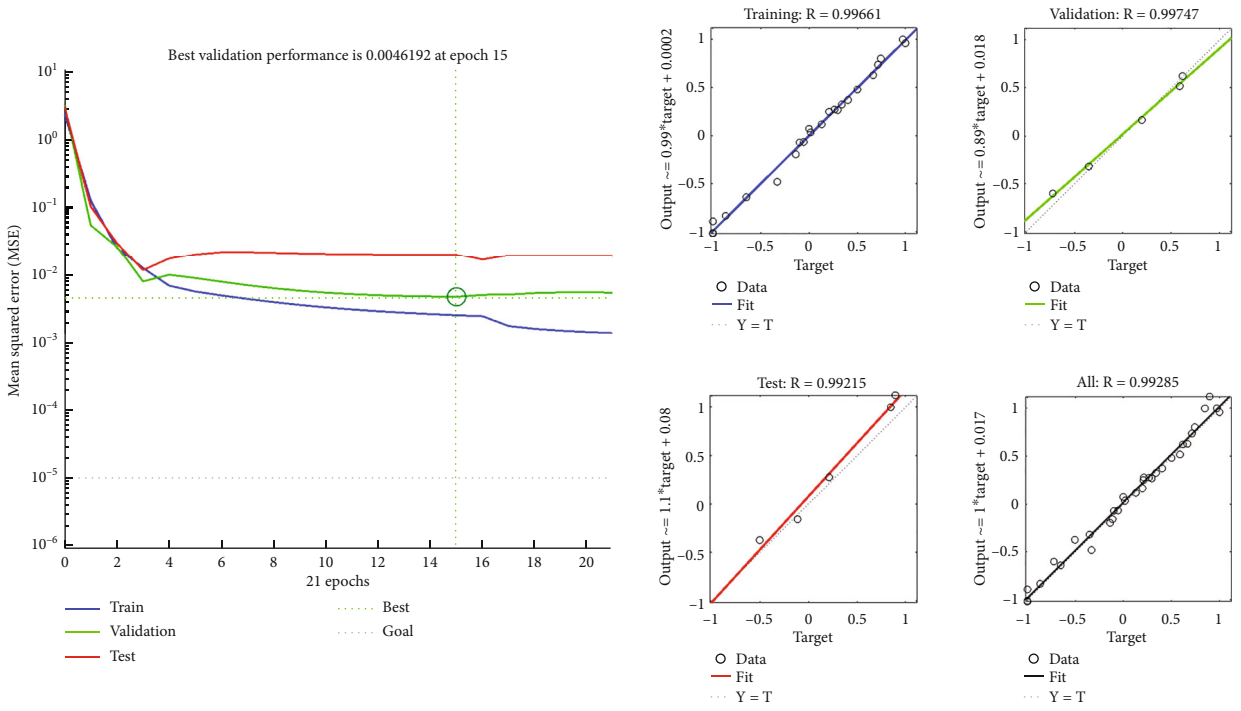

(TBARS)

Figure 3: Results of the BP neural network for the training, validation, test, and all sets.

Table 5: Predicted and experimental values of the POV and TBARS level and their relative errors for AkS at 37°C.

Indicators	POV (g/100 g)					TBARS (mg/kg)				
Storage time (d)	Experimental values	Predicted values (Arrhenius model)	Relative errors (%)	Predicted values (BP neural network model)	Relative errors (%)	Experimental values	Predicted values (Arrhenius model)	Relative errors (%)	PV (BP neural network)	Relative errors (%)
0	0.03	0.03	3.62	0.03	1.25	0.74	0.96	29.28	0.73	0.88
7	0.04	0.05	7.86	0.04	7.36	0.96	1.00	4.65	0.91	5.06
14	0.05	0.06	23.64	0.05	4.19	1.03	1.05	1.94	1.02	1.38
21	0.07	0.08	14.42	0.06	5.90	1.07	1.10	2.84	1.09	2.26
28	0.08	0.09	15.33	0.09	9.61	1.16	1.14	-1.72	1.15	0.86
35	0.11	0.10	-5.85	0.11	2.59	1.23	1.19	-3.27	1.22	0.59
42	0.13	0.12	-8.06	0.14	3.84	1.30	1.24	-4.82	1.31	0.56
49	0.14	0.13	-4.47	0.15	4.17	1.35	1.29	-4.47	1.33	1.17
56	0.15	0.15	-0.82	0.15	1.39	1.36	1.33	-2.11	1.38	1.52
63	0.16	0.16	4.97	0.16	0.08	1.39	1.38	-0.46	1.39	0.62
70	0.16	0.18	9.38	0.16	2.67	1.39	1.43	2.28	1.41	1.03

Table 6: Predicted and experimental shelf life of POV and TBARS and their relative errors for AkS at 37°C.

Indicators	EV (d)	PV (Arrhenius)	Relative errors (%)	PV (BP neural network)	Relative errors (%)
POV (d)	119	101	-15.13	133	11.76
TBARS (d)	142	183	28.87	161	13.39

4. Conclusions

The quality fluctuations of AkS at different storage temperatures were investigated in this study. Color differences, moisture content, acid value, peroxide value, TBARS level, aerobic plate count, and sensory scores were among these changes. Kinetic and BP neural network models were created to predict the quality fluctuations and shelf life of AkS. The predictive performances of the two models were assessed based on the projected outcomes.

High storage temperatures hasten the deterioration of AkS quality indices, such as $a*$ and $b*$values, AV, POV, and TBARS levels. In 70 d, the aerobic plate count did not change substantially ($P > 0.05$). The major source of degradation during storage was the oxidation of AkS, and the POV and TBARS level were chosen as indicators for the two models, and the quality indices of AkS were significantly correlated. The POV and TBARS level experimental results fit well with the two models. The Arrhenius model failed to effectively forecast POV quality changes on days 14, 21, and 28. In terms of quality change prediction, the relative error of the BP neural network model was less than 10%. In addition, the BP neural network model exhibited a lower error in predicting the shelf life of AkS, which was 11.76% for POV and 13.39% for TBARS level, respectively. Compared with the Arrhenius model, the BP neural network model demonstrated greater predicted performance and accuracy during the whole storage period. In conclusion, the BP neural network model can forecast the quality change and shelf life of AkS, which is expected to be low. As a result, further study employing hurdle technology, such as controlling water activity and adding antioxidants or food-grade additives, is required to extend the shelf life of AkS.

Data Availability

The data used to support the findings of this study are available from the corresponding author (Prof. Wei Kang) upon request.

Conflicts of Interest

The authors declare that there is no conflict of interest regarding the publication of this paper.

Acknowledgments

This work was supported by the National Key R&D Program of China (2023YFD2401200) and the National Natural Science Foundation of China (grant number 32001624).

References

[1] X. Yang, Y. Shi, Y. Cai, and H. Chi, "Quality changes and safety evaluation of ready-to-eat roasted Antarctic krill (*Euphausia superba*) during storage at room temperature (25°C)," *Journal of Ocean University of China*, vol. 22, no. 1, pp. 235–241, 2023.

[2] T. Suzuki and N. Shibata, "The utilization of Antarctic krill for human food," *Food Review International*, vol. 6, no. 1, pp. 119–147, 1990.

[3] Y. F. Li, Q. H. Zeng, G. Liu et al., "Food-grade emulsions stabilized by marine Antarctic krill (*Euphausia superba*) proteins with long-term physico-chemical stability," *LWT-Food Science and Technology*, vol. 128, article 109492, 2020.

[4] J. C. Gigliotti, J. Jaczynski, and J. C. Tou, "Determination of the nutritional value, protein quality and safety of krill protein concentrate isolated using an isoelectric solubilization/precipitation technique," *Food Chemistry*, vol. 111, no. 1, pp. 209–214, 2008.

[5] D. W. Sun, C. Cao, B. Li et al., "Antarctic krill lipid extracted by subcritical n-butane and comparison with supercritical CO_2 and conventional solvent extraction," *LWT-Food Science and Technology*, vol. 94, pp. 1–7, 2018.

[6] M. X. Ge, R. P. Chen, L. Zhang, Y. M. Wang, C. F. Chi, and B. Wang, "Novel Ca-chelating peptides from protein hydrolysate of Antarctic krill (*Euphausia superba*): preparation, characterization, and calcium absorption efficiency in CaCo-2 cell monolayer model," *Marine Drugs*, vol. 21, no. 11, p. 579, 2023.

[7] S. Nicol, J. Foster, and S. Kawaguchi, "The fishery for Antarctic krill – recent developments," *Fish and Fisheries*, vol. 13, no. 1, pp. 30–40, 2012.

[8] J. Sun and X. Mao, "An environmental friendly process for Antarctic krill (*Euphausia superba*) utilization using fermentation technology," *Journal of Cleaner Production*, vol. 127, pp. 618–623, 2016.

[9] Y. Z. Wang, Y. Q. Zhao, Y. M. Wang et al., "Antioxidant peptides from Antarctic krill (*Euphausia superba*) hydrolysate: preparation, identification and cytoprotection on H_2O_2-induced oxidative stress," *Journal of Functional Foods*, vol. 86, article 104701, 2021.

[10] B. Yoshitomi, "Utilization of Antarctic krill for food and feed," *Developments in Food Science*, vol. 42, pp. 45–54, 2004.

[11] M. Yu, Y. C. Fan, S. J. Xu et al., "Effects of antioxidants on the texture and protein quality of ready-to-eat abalone muscles during storage," *Journal of Food Composition and Analysis*, vol. 108, article 104456, 2022.

[12] X. Sun, L. L. Zhu, Q. Xin et al., "Cleavage sites and non-enzymatic self-degradation mechanism of ready-to-eat sea cucumber during storage," *Food Chemistry*, vol. 375, article 131722, 2022.

[13] D. Y. Li, Z. Yuan, Z. Q. Liu et al., "Effect of oxidation and Maillard reaction on color deterioration of ready-to-eat shrimps during storage," *LWT-Food Science and Technology*, vol. 131, article 109696, 2020.

[14] A. M. Ndob and A. Lebrt, "Prediction of pH and aw of pork meat by a thermodynamic model: new developments," *Meat Science*, vol. 138, pp. 59–67, 2018.

[15] Y. Li, K. Zhong, X. Wang et al., "Sensory evaluation and model prediction of vacuum-packed fresh corn during long-term storage," *Foods*, vol. 12, no. 3, p. 478, 2023.

[16] Z. F. Wang, Z. F. He, D. Zhang, H. J. Li, and Z. M. Wang, "Using oxidation kinetic models to predict the quality indices of rabbit meat under different storage temperatures," *Meat Science*, vol. 162, article 108042, 2020.

[17] J. Y. Han, M. J. Kim, S. D. Shim, and S. J. Lee, "Application of fuzzy reasoning to prediction of beef sirloin quality using time temperature integrators (TTIs)," *Food Control*, vol. 24, no. 1-2, pp. 148–153, 2012.

[18] E. Torrieri, F. Russo, M. R. Di, S. Cavella, F. Villani, and F. Masi, "Shelf life prediction of fresh Italian pork sausage modified atmosphere packed," *Food Science and Technology International*, vol. 17, no. 3, pp. 223–232, 2011.

[19] J. Y. Choi, H. J. Lee, J. S. Cho, Y. M. Lee, J. H. Woo, and K. D. Moon, "Prediction of shelf-life and changes in the quality characteristics of semidried persimmons stored at different temperatures," *Food Science and Biotechnology*, vol. 26, pp. 1255–1262, 2017.

[20] M. Khajeh and A. Barkhordar, "Modelling of solid-phase tea waste extraction for the removal of manganese from food samples by using artificial neural network approach," *Food Chemistry*, vol. 141, no. 2, pp. 712–717, 2013.

[21] M. B. Takahashi, H. D. Oliveira, E. F. Nunez, and J. C. Rocha, "Brewing process optimization by artificial neural network and evolutionary algorithm approach," *Journal of Food Process Engineering*, vol. 42, no. 5, 2019.

[22] Z. T. Fu, S. Zhao, X. S. Zhang, M. Polovka, and X. Wang, "Quality characteristics analysis and remaining shelf life prediction of fresh Tibetan Tricholoma matsutake under modified atmosphere packaging in cold chain," *Food*, vol. 8, no. 4, pp. 136–150, 2019.

[23] N. Zhu, K. Wang, S. L. Zhang, B. Zhao, J. N. Yang, and S. W. Wang, "Application of artificial neural networks to predict multiple quality of dry-cured ham based on protein degradation," *Food Chemistry*, vol. 344, article 128586, 2021.

[24] J. S. Kim, F. Shahidi, and M. S. Heu, "Tenderization of meat by salt-fermented sauce from shrimp processing by-products," *Food Chemistry*, vol. 93, no. 2, pp. 243–249, 2005.

[25] S. Rønholt, A. S. Madsen, J. J. Kirkensgaard, K. Mortensen, and J. C. Knudsen, "Effect of churning temperature on water content, rheology, microstructure and stability of butter during four weeks of storage," *Food Structure*, vol. 2, no. 1-2, pp. 14–26, 2014.

[26] H. H. Harrison and J. L. Watts, "Lipid extraction and analysis," *Methods in Molecular Biology*, vol. 2468, pp. 271–281, 2022.

[27] Y. J. Guo, X. Liang, J. M. Bi et al., "A polyamidoamine-mediated competitive colorimetric assay based on gold nanoparticles for determining acid values in edible sunflower seed, corn and extra virgin olive oils," *Food Chemistry*, vol. 285, pp. 450–457, 2019.

[28] N. Cebi, M. T. Yilmaz, O. Sagdic, H. Yuce, and E. Yelboga, "Prediction of peroxide value in omega-3 rich microalgae oil by ATR-FTIR spectroscopy combined with chemometrics," *Food Chemistry*, vol. 225, pp. 188–196, 2017.

[29] W. J. Fan, Y. L. Chi, and S. Zhang, "The use of a tea polyphenol dip to extend the shelf life of silver carp (Hypophthalmicthys molitrix) during storage in ice," *Food Chemistry*, vol. 108, no. 1, pp. 148–153, 2008.

[30] Y. N. Liu, S. M. Zhao, F. Guan, and Y. Yuan, "Establishment of a model for evaluating shelf life of Pseudosciaena crocea in simulated logistics and storage," *Journal of Food Protection*, vol. 84, no. 7, pp. 1188–1193, 2021.

[31] L. A. Escalona-garcía, R. Pedroza-islas, R. Natividad, M. E. Rodríguez-Huezo, H. Carrillo-Navas, and C. Pérez-Alonso, "Oxidation kinetics and thermodynamic analysis of chia oil microencapsulated in a whey protein concentrate-polysaccharide matrix," *Journal of Food Engineering*, vol. 175, pp. 93–103, 2016.

[32] Y. F. Sun, H. T. Chang, and Z. J. Miao, "Research on BP neural network model for water demand forecasting and its application," *Applied Mechanics and Materials*, vol. 170-173, pp. 2352–2355, 2012.

[33] M. Ran, L. P. He, C. Q. Li, Q. J. Zhu, and X. F. Zeng, "Quality changes and shelf-life prediction of cooked cured ham stored

at different temperatures," *Journal of Food Protection*, vol. 84, no. 7, pp. 1252–1264, 2021.

[34] X. F. Xia, B. H. Kong, J. Liu, X. P. Diao, and Q. Liu, "Influence of different thawing methods on physicochemical changes and protein oxidation of porcine longissimus muscle," *LWT-Food Science and Technology*, vol. 46, no. 1, pp. 280–286, 2012.

[35] A. Singh, A. Mittal, and S. Benjakul, "Undesirable discoloration in edible fish muscle: Impact of indigenous pigments, chemical reactions, processing, and its prevention," *Comprehensive Reviews in Food Science and Food Safety*, vol. 21, no. 1, pp. 580–603, 2022.

[36] A. M. Cassens, A. N. Arnold, R. K. Miller, K. B. Gehring, and J. W. Savell, "Impact of elevated aging temperatures on retail display, tenderness, and consumer acceptability of beef," *Meat Science*, vol. 146, pp. 1–8, 2018.

[37] I. Chelh, P. Gatellier, and V. Sante-lhoutellier, "Characterisation of fluorescent Schiff bases formed during oxidation of pig myofibrils," *Meat Science*, vol. 76, no. 2, pp. 210–215, 2007.

[38] M. Petracci, M. Bianchi, S. Mudalal, and C. Cavani, "Functional ingredients for poultry meat products," *Trends in Food Science and Technology*, vol. 33, no. 1, pp. 27–39, 2013.

[39] C. R. Ren, G. Q. Huang, S. Q. Wang et al., "Influence of atmospheric pressure argon plasma treatment on the quality of peanut oil," *European Journal of Lipid Science and Technology*, vol. 119, no. 11, article 1600513, 2017.

[40] J. A. Hernández Becerra, A. A. Ochoa Flores, G. Valerio-Alfaro, I. Soto-Rodriguez, M. T. Rodríguez-Estrada, and H. S. García, "Cholesterol oxidation and astaxanthin degradation in shrimp during sun drying and storage," *Food Chemistry*, vol. 145, pp. 832–839, 2014.

[41] I. Soto-Rodríguez, P. Campillo-Velázquez, J. Ortega-Martínez, M. Rodríguez-Estrada, G. Lercker, and H. S. Garcia, "Cholesterol oxidation in traditional Mexican dried and deep-fried food products," *Journal of Food Composition and Analysis*, vol. 21, no. 6, pp. 489–495, 2008.

[42] C. L. Qu, X. K. Wang, Z. W. Wang, S. C. Yu, and D. X. Wang, "Effect of drying temperatures on the peanut quality during hot air drying," *Journal of Oleo Science*, vol. 69, no. 5, pp. 403–412, 2020.

[43] G. L. Di, P. R. Salgado, and A. N. Mauri, "Encapsulation of fish oil in soybean protein particles by emulsification and spray drying," *Food Hydrocolloids*, vol. 87, pp. 891–901, 2019.

[44] K. K. Radha, S. Babuskin, S. B. Azhagu et al., "Antimicrobial and antioxidant effects of spice extracts on the shelf life extension of raw chicken meat," *International Journal of Food Microbiology*, vol. 171, pp. 32–40, 2014.

[45] D. Y. Li, H. K. Xie, Z. Y. Liu et al., "Shelf life prediction and changes in lipid profiles of dried shrimp (*Penaeus vannamei*) during accelerated storage," *Food Chemistry*, vol. 297, article 124951, 2019.

[46] J. Du, M. Zhang, L. H. Zhang, C. L. Law, and L. Kun, "Shelf-life prediction and critical value of quality index of Sichuan sauerkraut based on kinetic model and principal component analysis," *Food*, vol. 11, no. 12, pp. 1762–1781, 2022.

[47] F. Kaymak-Ertekin and A. Gedik, "Kinetic modelling of quality deterioration in onions during drying and storage," *Journal of Food Engineering*, vol. 68, no. 4, pp. 443–453, 2005.

[48] H. K. Zhu, Y. Ye, H. F. He, and C. W. Dong, "Evaluation of green tea sensory quality via process characteristics and image information," *Food and Bioproducts Processing*, vol. 102, pp. 116–122, 2017.

[49] R. M. Dahlquist-Willard, M. N. Marshall, S. L. Betts, C. C. Tuell-Todd, J. S. VanderGheynst, and J. J. Stapleton, "Development and validation of a Weibull–Arrhenius model to predict thermal inactivation of black mustard (Brassica nigra) seeds under fluctuating temperature regimens," *Biosystems Engineering*, vol. 151, pp. 350–360, 2016.